J Therm Anal Calorim (2012) 109:1347–1351
DOI 10.1007/s10973-012-2321-7

The impact of drying phenomena and heat treatment on the structure of porous silicon

A. Ould-Abbas · M. Bouchaour · D. Trari · N. E. Chabane Sari

Received: 2 May 2011 / Accepted: 7 February 2012 / Published online: 28 March 2012

Abstract Porous silicon (PS) has received a great deal of attention due to its light emitting properties. This characteristic has led to a wide range of applications (optoelectronic devices, physical and chemical sensors, solar cells…). Indeed, this material is a good candidate for improving the ratio quality/price of solar cells. Its fabrication needs anodisation of single crystalline silicon in a mixture of HF/methanol solution. In order to simulate the different steps needed to "develop" the solar cells, PS layers (single or two layers) were subjected to different annealing. In this article, we discuss the influence of drying and annealing on the morphology of PS. SEM observations and gravimetric measurements are reported.

Keywords Porous Silicon · Drying · Heat Treatments · SEM · Morphology

Introduction

Porous silicon (PS) was known for scientists since 1950s. In 1956, Uhlirs [1] revealed a microstructure form of silicon, it was a black film on the surface of wafers. The porous nature of this film was studied by Turner [2] and confirmed by Watanabe [3].

The first uses of porous silicon were in the field of Silicon on insulator (SOI). Then in 1990, Canham [4], Lehman and Gösele [5] discovered the photoluminescence properties of PS. This discovery leads to several applications of this material. PS is used in the photovoltaic field as anti-reflective layers [6] or as sacrificial layers as proposed by Bergmann [7] and Tayanaka [8]. In the realization of solar cells, we applied the following steps of heat treatments of PS at different atmospheres:

– First, PS is annealed in hydrogen at the temperature of 450° C for 15 min to desorb the porous silicon, then we change the temperature at 950° C and we let it for 2 h to simulate the step of liquid phase epitaxy (LPE) [9].
– After it is annealing at 1,000° C for 1 h under nitrogen atmosphere for the simulation and the development of the junction and then at 700° C for 30 s in air for the contacts.

In this study, we present a detailed study of PS. The relationship between morphology and heat treatment and drying is clarified.

Experimental procedure

We obtain porous structures by anodic treatment of silicon (Si). We use 0.01–0.025 ohm cm^{-1}, boron doped (100) or (111) Si wafers. We choose this category because of its highest doping and thus, we do not need ohmic contact at backside.

Electrochemical anodisation

In order to get the mesoporous silicon (diameter of pores in the range 10–50 nm), we made an electrochemical anodisation. The samples are obtained from the anodisation of single crystalline silicon in HF (48%): C_2H_5OH – 1:1. The anodisation current ranges between 5 and 75 mA cm^{-2}, while the anodisation time ranges between 1 and 20 min.

A. Ould-Abbas (✉) · M. Bouchaour · D. Trari · N. E. Chabane Sari
Département de Physique, Laboratoire de Matériaux & Energies Renouvelables, Faculté des Sciences, Université AbouBakr Belkaid, B. P 119, Tlemcen 13000, Algérie
e-mail: aouldabbes@yahoo.fr

Current density permits to obtain different porosities. Indeed, a low current density led to a low porosity and inversely. However, with the anodisation time, we get the thickness of the porous layer needed. Ethanol is added to the HF solution to improve the wettability of the acid and to allow F–ions to diffuse into the pores. The anodisation is performed in a double tank cell (Fig. 1) with electrolytic front and back-side contacts separated by the silicon wafer.

The two Au electrodes are connected to a current generator. To minimize the effects of hydrogen bubbles formed during the anodisation, an agitator can be placed in the half-cell. After this step, the samples obtained are rinsed in deionised water and are dried under nitrogen atmosphere.

Drying of PS samples

Different approaches have been proposed in the recent past to avoid the destructive effects of drying. One common characteristic of as-prepared porous silicon is its tendency to deform and crack during drying. This is generally undesirable in terms of the mechanical stability and thus in the quality of the material. One of these techniques is the supercritical drying.

Heat treatment

After the last step, we anneal first the samples at 450° C for 15 or 30 min in a hydrogen atmosphere and then we change the temperature to 950° C for 2 h. We repeat this last step (i.e., 950° C) in a neuter atmosphere to compare the effect of the atmosphere in annealing. We do again the annealing at 1,000° C for 1 h, in nitrogen atmosphere. This stage led us to simulate the diffusion of dopants for n^+/p junction. Finally, we anneal at 700 °C in air to simulate the step of contacts realization.

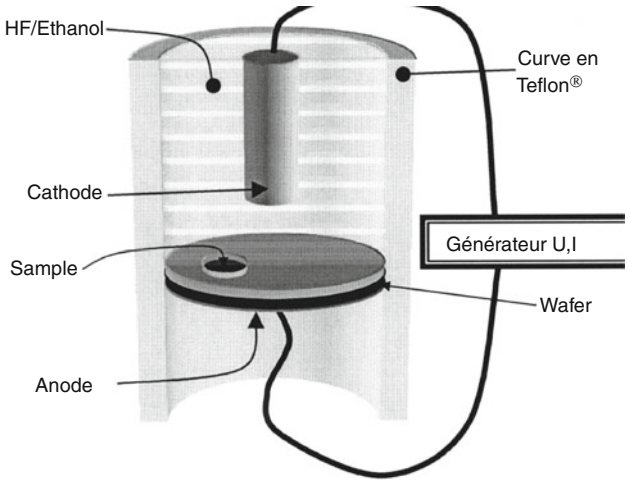

Fig. 1 The anodisation double tank cell with electrolytic front and backside contacts separated by the silicon wafer

The surface morphology of the samples was examined by scanning electron microscopy (SEM). The thicknesses were evaluated by the cross-sectional SEM analysis and the porosity was measured by gravimetric method. To determine the size of the pores we use the technique of adsorption and gas desorption, also let us note that the porosity of the layers is determined by this method.

Results and discussion

Gravimetry

Figure 2 shows the measurement of the porosity by gravimetric method. The porosity changes with the current density. In fact, the porosity is given by Eq. 1. The substrates of silicon were weighed.

$$p = \frac{m_1 - m_2}{m_1 - m_3} \quad (1)$$

where m_1 is the mass before anodisation, m_2 is the mass after anodisation, and m_3 is the mass after leaving the porous layer by immersion of the wafer in KOH solution.

With our experimental conditions, we obtain $p = 24 \pm 8\%$ for current density $J = 5$ mA cm^{-2} and $p = 50 \pm 8\%$ for $J = 75$ mA cm^{-2}.

Nitrogen adsorption measurements

Nitrogen isotherms for the PS sample obtained with a density of current of 75 mA/cm^2 has a sharp hysteresis loop (see Fig. 3, left), reflecting capillary condensation of adsorbate in the uniform mesopores channels, and evaporation step related to the evacuation of adsorbate from the pores. Thus, a framework of these materials has a uniform array of mesopores with the same diameter a. From this curve, we determine the specific surface determined by BET method [10, 11] and

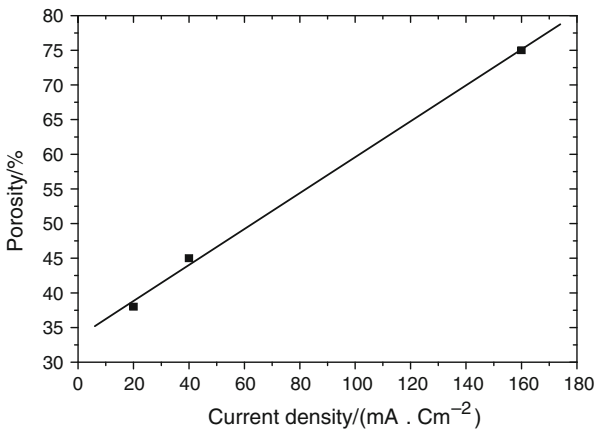

Fig. 2 PS (111) porosity plot with current density

Table 1 Structural and adsorption characteristics of the sample obtained with current density of 75 mA/cm^2

$S_{BE}/m^2/g^{-1}$	$V_{BJH}/cm^3/g^{-2}$	d_{BJH}/nm	*P* (porosity)/%
5.36	0.01	6.9	48.5

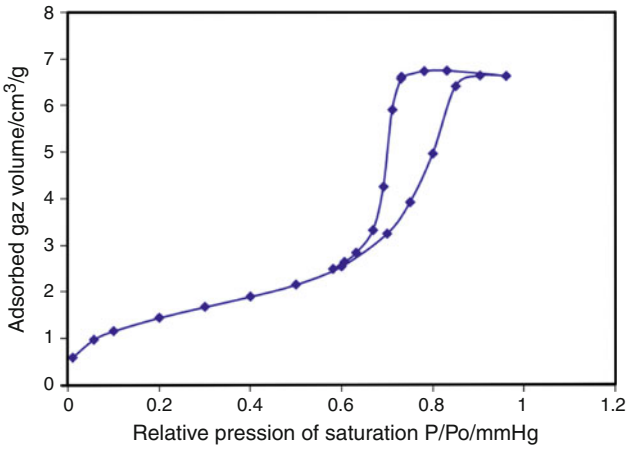

Fig. 3 Gas adsorption isotherm of porous silicon ($J = 75$ mA/cm^2, $t = 10$ min in 48% HF/EtOH electrolyte)

average pore size by BJH method [10, 12] (based on the volume of gas absorbed by the sample).

The properties of the porous structures are summarized in Table 1 see Fig. 3.

Drying characterization

In Figures 4 and 5, we give an example of cracking pattern of PS. It has been reported several times that the formation of PS, with high porosity and/or thickness, leads systematically to cracking of the layer during the evaporation of the solvent. An important step in the fabrication process of high quality PS layers is the drying method employed immediately after the etching of the wafer [13, 14]. The origin of the cracking is the large capillary stress associated with evaporation from the pores. During the evaporation a gas/liquid interface forms inside the pores and a pressure drop Δp across the gas/liquid interface occurs. Δp is given by:

$$\Delta P = 2\gamma_{LV}/r \quad (2)$$

where ΔP is the difference of pressure between liquid and vapor phase, γ_{LV} is the liquid vapor tension of the fluid, and r is the capillary radius.

The cracking appeared in Fig. 4 is showed by the white stripe of critical thickness given by h_c (Eq. 3).

$$h_c = (r/\gamma_{LV})^2 E_{si}(1-p)\gamma_{si} \quad (3)$$

where γ_{LV} is the surface tension, γ_{LV} superficial tension, p is the porosity, r is pore's radius, and E_{si} are the smallest modulus of porosity of PS.

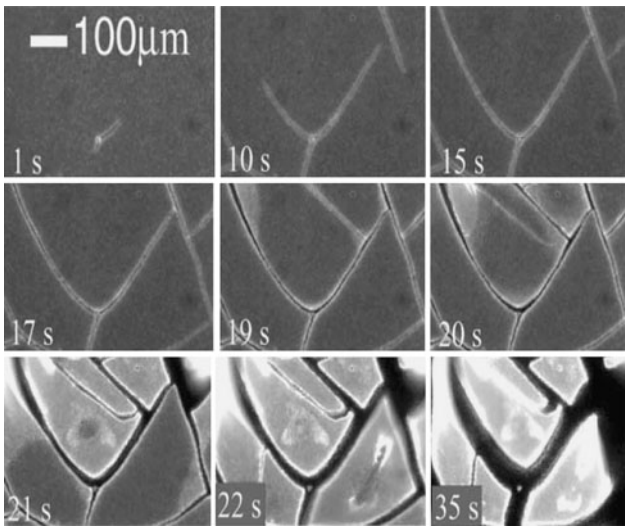

Fig. 4 SEM images of a 12 mA/10 min PS sample during drying [13]

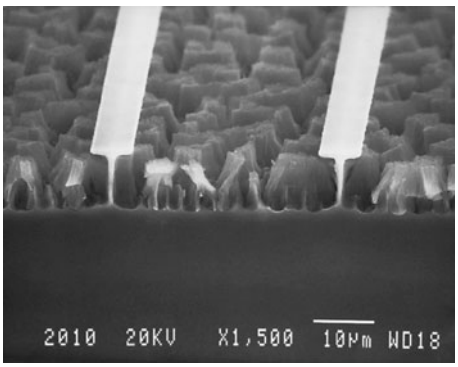

Fig. 5 Cross-sectional SEM image of typical cracking pattern. The *white stripes* are due to crystalline Si after etching [14]

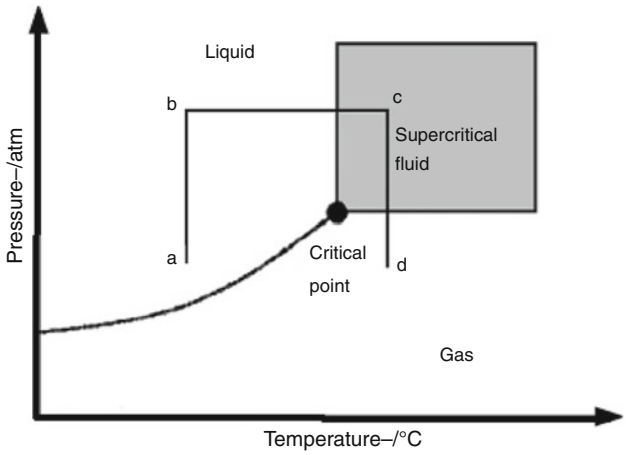

Fig. 6 Schematic phase diagram showing pressure–temperature paths used in supercritical drying

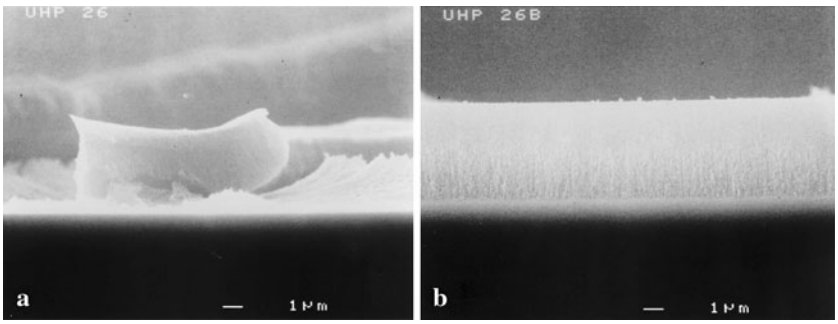

Fig. 7 **a** SEM observation of a 5 µm thick p^+-type porous silicon layer (porosity of 95%) dried in ambient air. **b** SEM observation of a 5 µm thick p^+-type porous silicon layer (porosity of 95%) dried with supercritical CO_2

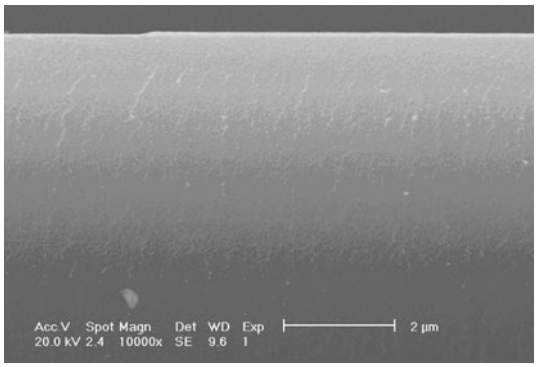

Fig. 8 Porous structure (single layer of porosity of 20%) before annealing in hydrogen atmosphere at 950 °C

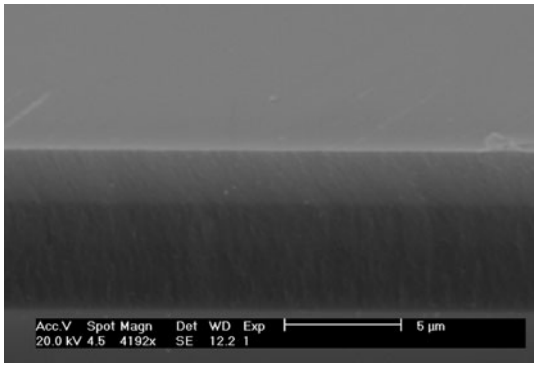

Fig. 10 Porous structure (double layer of porosity of 20%) before annealing in hydrogen atmosphere at 1,050 °C

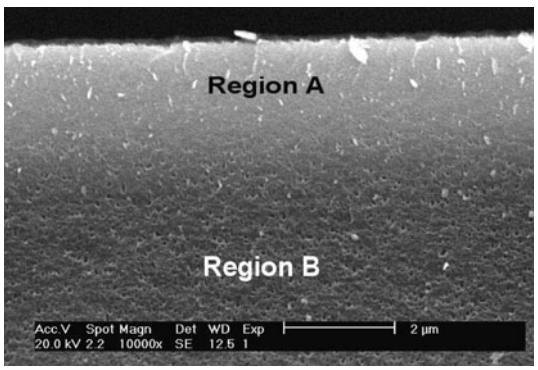

Fig. 9 Porous structure (single layer of porosity of 20%) after annealing in hydrogen atmosphere at 950 °C

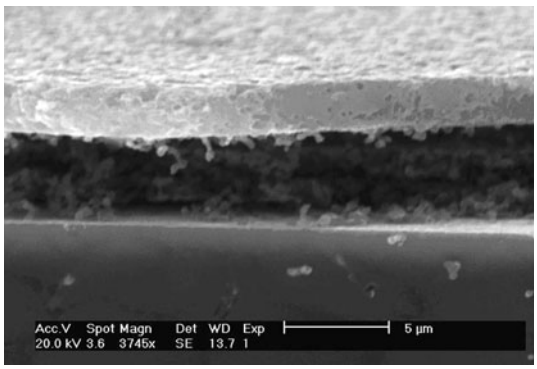

Fig. 11 Porous structure (double layer of porosity of 20%) after annealing in hydrogen atmosphere at 1,050 °C

The supercritical drying technique has been proposed in the recent past to avoid the destructive effects of air-drying. This technique is based on the exploitation of the fact that when the pressure is raised the interface between the liquid and the gas phase becomes unstable, when the pressure is larger than the critical pressure the interface gas/liquid disappears, and a mixture of the two phases appears (supercritical fluid). This is the most efficient drying method. In such technique, HF solution is replaced by a suitable "liquid", usually carbon dioxide, under high pressure [15]. The phase is then moved above the critical point by raising the pressure and temperature, as schematically shown in Fig. 6 [16] path a–b and b–c. Then, the supercritical liquid (path a–b and c–d) removes the gas. This drying procedure allows to produce layers with very high thickness and porosity values (up to 95%) improving the optical flatness and the homogeneity as well.

Figure 7 presents a comparison between SEM observations of air-drying and supercritical drying with supercritical CO_2 of a 5 µm thick p^+-type PS layer (porosity of 95%) [17].

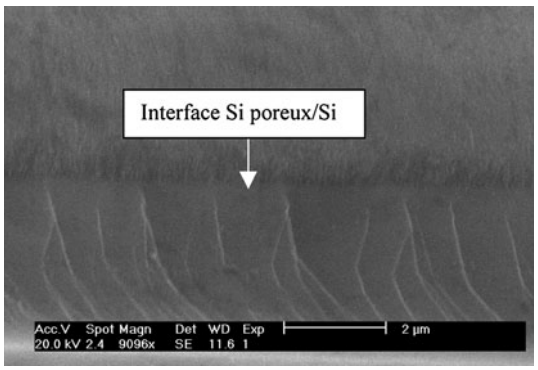

Fig. 12 Porous structure (double layer of porosity of 20%) after annealing in nitrogen atmosphere at 1,050° C

Heat treatment

Figures 8, 9, and 10 present SEM observations of effect of heat treatment on the morphology of porous layers. The morphology of PS changes after annealing in hydrogen atmosphere. We detect a tendency to crystallization on the surface (on 2–3 µm from the surface as shown in Fig. 9 (area A)). We observe also, a microstructural modification in the area B. It represents the coalescence of pores.

PS (111) undergo the same changes as PS (100). M. Banerjee [18] confirms our observations. We enhance the time and the temperature to desorb PS. We observe a homogeneous surface as shown in Fig. 11 with this augmentation of the time and the temperature.

The results further demonstrate that the top low porosity layer is recrystallized into quasi-mono-crystalline porous silicon (QMPS) layer after thermal annealing [19].

We do not observe any modification of the structure when we anneal PS in nitrogen or in air (these steps for the simulation of the realization of the solar cell contacts) (Fig. 12).

Conclusions

In this article, we presented the electrochemical anodisation done on p-type Si (100) and (111) substrate with different time and current densities. We determined the pores' size, porosity, and specific surface by gravimetric method. This one revealed the cylindrical form of the pores. We discussed the impact of drying and heat treatment on the surface of PS. Drying step allowed to obtain a good and homogeneous layers. Modification of morphology was observed when samples were annealed. Surface analysis of low porosity (20–30%) porous silicon films produced by electrochemical anodization of heavily doped p-Si and thermally annealed at the temperature range 950–1,050 °C in pure hydrogen is reported in this study. The analysis showed that at high temperature, PS crystallized. SEM observation illustrated that porous silicon was transformed into quasi-monocrystalline porous silicon (QMPS) with the surface more or less pore free and few voids embedded inside the body. All these steps allowed us to elaborate silicon thin films solar cells.

References

1. Uhlir A. Electronic shaping of germanium and silicon. Bell Syst Tech J. 1956;35:333–47.
2. Turner DR. Electropolishing silicon in hydrofluoric acid solutions. J Electrochem Soc. 1958;105:402–7.
3. Watanabe Y, Sakai T. Application of thick anode film to semiconductor devices. Rev Electron Commun Labs. 1971;19:899–903.
4. Canham LT. Silicon quantum wire array fabrication by electromechanical and chemical dissolution of wafers. Appl Phys Lett. 1990;57:1046.
5. Lehman V, Gösele U. Porous silicon formation: a quantum wire effect. Appl Phys Lett. 1991;58:856–9.
6. Bilyalov R. R., Lautenschlager H., Schetter C.et al. Porous silicon as an antireflection coating for multicrystalline solar cells. In: Proc. of 14th European photovoltaic solar energy conference, Barcelona, Spain, 1997, 788–791.
7. Werner J. H., Bergman R. B., Technical digest of international PVSEC-11, Sapporo, 1999, p. 923.
8. Tayanaka H., Yamauchi K., Matsushita T. Thin film crystalline silicon solar cells obtained by separation of a porous silicon sacrificial layer. Proc. of 2nd world conference and exhibition on photovoltaic solar energy conversion, Vienna, Austria, 1998, 1272–1277.
9. Ould-abbas A, Bouchaour M, Chabane-Sari N-E, Berger S, Kaminski A, Fave A. Growth of silicon thin film by LPE on porous silicon bilayers. J Therm Anal Calorim. 2004;76:685–91.
10. Barczak M, Oszust-Cieniuch M, Borowski P, Fekner Z, Zieba E. SBA-15 silicas containing sucrose. Chemical, structural and thermal studies. J Therm Anal Calorim. 2011. doi:10.1007/s109730111973.
11. Brunauer JS, Emmett PH, Teller E. Adsorption of gases in multimolecular layers. J Am Chem Soc. 1938;60:309–19.
12. Barrett EP, Joyner LG, Halenda P. The determination of pore volume and area distributions in porous substances. I. Computations from nitrogen isotherms. J Am Chem Soc. 1951;73:373–80.
13. Bellet D, Canham L. Controlled drying: the key to better quality porous semiconductors. Adv Mater. 1998;10(6):487–90.
14. C. Vinegoni, M. Cazzanelli and L Pavesi, Manuscript redacted at University of Pittsburgh, USA. October 2000.
15. Bouchaour M, Ould-Abbes A, Diaf N, Chabane Sari N. The role of supercritical CO_2 in the drying of porous silicon. J Therm Anal Calorim. 2004;76:677–84.
16. Canham LT, Cullis AG, Pickering C, Dosser OD, Cox TI, Lynch TP. Luminescent anodized silicon aerocrystal networks prepared by supercritical drying. Nature. 1994;368:133.
17. Bisi O, Ossicini S, Pavesi I. Porous silicon: a quantum sponge structure for silicon based optoelectronics. Surf Sci Rep. 2000;38:1–126.
18. Banerjee M, Bontempi E, Tyagi AK, Basu S, Saha H. Surface analysis of thermally annealed porous silicon. Appl Surf Sci. 2008;2541:837–41.
19. Hong cai a, Honglie shen, Lei zhang, Haibin huang, Linfeng lu, Zhengxia tang, Jiancang shen. Silicon epitaxyon textured double layer porous silicon by lpcvd. Phys B. 2010;405:3852–6.